

Dynamical Photon Condensation into Wannier-Stark States

Arkadiusz Kosior , Karol Gietka , Farokh Mivehvar , and Helmut Ritsch 
Institut für Theoretische Physik, Universität Innsbruck, A-6020 Innsbruck, Austria

Strongly coupled light-matter systems can exhibit nonequilibrium collective phenomena due to loss and gain processes on the one hand and effective photon-photon interactions on the other hand. Here we study a photonic lattice system composed of a linear array of driven-dissipative coupled cavities (or cavity modes) with linearly increasing resonance frequencies across the lattice. The model amounts to a driven-dissipative Bose-Hubbard model in a tilted potential *without* the particle-conservation constraint. We predict a diverse range of stationary and non-stationary states resulted from the interplay of the tilt, tunneling, on-site interactions, and the loss and gain processes. Our key finding is that, under weak on-site interactions, photons mostly Bose condense into a selected, single-particle Wannier-Stark state, instead of exhibiting expected Bloch oscillations. As the strength of the photon-photon interactions increase, a non-stationary regime emerges which is marked surprisingly by periodic Bloch-type oscillations. These intriguing, nontrivial effects are a direct consequence of the driven-dissipative nature of the system.

Introduction.—In classical physics, matter and light appear as distinct entities. Matter is composed of elementary particles, while light is described as an electromagnetic wave. In quantum mechanics this sharp division between matter and light becomes less stringent owing to the particle-wave duality [1]. On the one hand, matter particles are assigned a de Broglie wavelength and can exhibit wave-like phenomena such as diffraction and interference. On the other hand, light is considered to be composed of discrete quanta—photons—which can exhibit particle-like behavior on detection. While direct photon-photon interaction is typically negligible, when sufficiently enhanced it can lead to intriguing collective phenomena in an analogy to correlated matter.

Nevertheless there is a major difference between massive many-particle and many-photon systems at low energy scales: while the matter-particle number is strictly conserved, photons can appear and disappear due to absorption, spontaneous or stimulated emission, and external photon sources. This causes open photonic systems to be inherently out of equilibrium [2] and even stationary states are typically not determined simply by temperature and entropy but rather by the dynamical balance of gain and loss. Intriguing nonequilibrium phenomena thus appear in composite light-matter systems [3–6] and in particular in quantum fluids of light [7]. The most notable example is the observation of the quasi-equilibrium Bose-Einstein condensate (BEC) of exciton polaritons—bosonic quasiparticles composed of a mixture of an exciton (an electron-hole pair) and a cavity photon—in a semiconductor microcavity [8–11] and the BEC of photons interacting via molecules in a multimode optical microcavity [12]. Despite the driven-dissipative nature of these systems, they still exhibit an effective thermalization process to which one can attribute an effective temperature. This stands in a sharp contrast to a typical laser operation, where the thermalization is completely ineffective and the photon gas is far out-of-equilibrium.

Substantial interest has been focused on the investiga-

tion of strongly correlated many-body effects with photons [13, 14]. In earlier investigations, the focus was on establishing connections between driven-dissipative steady states and equilibrium many-body phases. These included the prediction of a phase transition from a superfluid to a Mott-insulator state for photons via the photon-blockade effect in coupled cavities [15–21]. More recently the focus was shifted towards the intriguing realm of the driven-dissipative regime, where nonequilibrium steady-state phases exhibit distinct properties in comparison to thermally equilibrium cases [22–24]. For example, the boundary between monostable and bistable phases in a driven-dissipative model resembles characteristic Mott insulator lobes but the mean photon density is not constant within these regions [22]. In a wider context various ideas and schemes have also been put forward to simulate geometric phases and gauge potentials for photons, opening the possibility for realizing nonequilibrium topological photonic states [25, 26].

In this Letter, we investigate a driven-dissipative array of coupled Kerr cavities (or cavity modes) with linearly increasing resonant frequencies mimicking a 1D bosonic optical lattice subjected to an external force. In our generic model photons (bosons) are continuously injected into the system via a coherent pump to a selected cavity. Photons are then redistributed via nearest neighbor mode couplings until they eventually leak out through imperfect cavity mirrors. The dynamics of the system can be effectively captured by a driven-dissipative Bose-Hubbard model in a tilted potential *without* particle conservation. Despite the conceptual simplicity, the model, as we demonstrate, exhibits a variety of intriguing stationary and non-stationary, nonequilibrium phenomena controllable by the system parameters.

A central result of our study is that for sufficiently weak on-site interactions, photons dynamically condense due to the explicit $U(1)$ symmetry breaking into a selected, spatially-localized state (Fig. 1), instead of exhibiting expected Bloch oscillations [27, 28]. Specifically,

we show that the condensate wavefunction is often close to a single Wannier-Stark (WS) state with only small contributions from a few neighboring WS states; see Fig. 2. Intriguingly, by increasing the strength of local on-site interactions the system enters a non-stationary regime (Fig. 3) where the photon density undergoes periodic Bloch-type oscillations over time as shown in Fig. 4 [29–31]. This finding strongly contrasts with the irreversible decay of Bloch oscillations of interacting atoms in a 1D tilted lattice [32–36]. Let us emphasize here that both of these regimes appear independent of initial conditions and the choice of the pumped cavity, and are a direct consequence of the driven-dissipative nature of the system. As our model is quite generic, a corresponding experimental realization should be implementable in various platforms including superconducting circuits [37–39], photonic crystal structures [40], waveguide-coupled optical cavities [41], and atom-filled transverse multi-mode cavities [42].

Model and its Hamiltonian.—Consider a linear array of standing-wave coupled cavities (labeled by $j \in \mathbb{Z}$) with linearly increasing resonant frequencies $\omega_j \propto j$, each containing a Kerr-like non-linear medium. Coherent pumps with the frequency ω_p continuously inject photons into the cavity modes. Each cavity is coupled to two adjacent cavities due to the photon leakage through the cavity mirrors, which leads to a coherent hopping of photons in the cavity lattice. The Hamiltonian of the system in the rotating frame of the coherent pumps is given by [43],

$$\hat{H} = \sum_j \left[\hbar \Delta_j \hat{a}_j^\dagger \hat{a}_j - J (\hat{a}_j^\dagger \hat{a}_{j+1} + \text{H.c.}) + \chi \hat{a}_j^{\dagger 2} \hat{a}_j^2 \right] + \hbar \sum_j \eta_j (\hat{a}_j + \hat{a}_j^\dagger), \quad (1)$$

with $\hat{a}_j, \hat{a}_j^\dagger$ being bosonic operators annihilating and creating a photon in the j -th cavity, respectively. Here we have defined

$$\Delta_j = \omega_j - \omega_p \equiv \Delta\omega (j - j_0), \quad (2)$$

as the cavity-pump detuning. Moreover, J is the nearest-neighbor photon tunneling-amplitude rate, χ the on-site photon-photon interaction strength due to the effective Kerr non-linearity, and η_j the pumping rate of the j -th cavity. Photon losses, assumed to be the same for all the cavities, κ are taken into account via the quantum Heisenberg equations of motion,

$$\frac{d\hat{a}_j}{dt} = \frac{i}{\hbar} [\hat{H}, \hat{a}_j] - \kappa \hat{a}_j. \quad (3)$$

The first line of the Hamiltonian (1) describes the familiar equilibrium Bose-Hubbard model in a tilted lattice. While in the non-interacting limit the equilibrium model features well-known Bloch oscillations [27, 28], it has been recently shown that strong interactions can lead

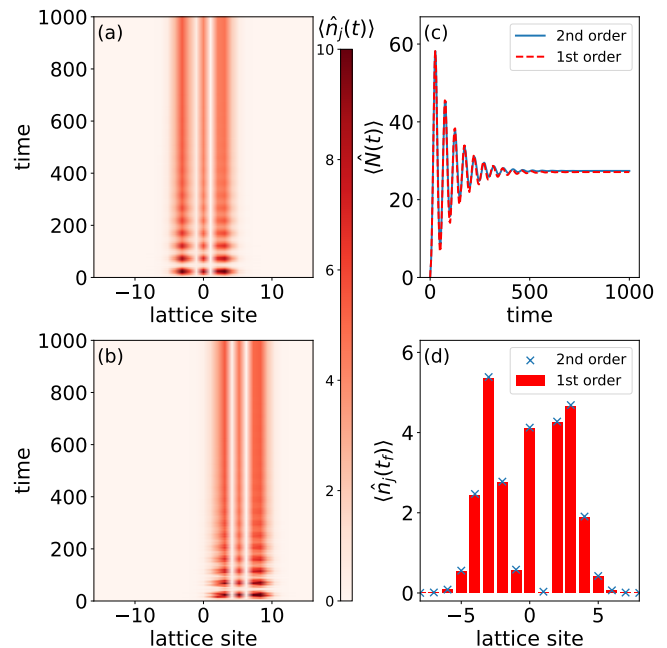


FIG. 1. Nonequilibrium dynamics of the system for a weak photon-photon interaction strength $\chi = 10^{-2}$ and the lattice tilt $\Delta\omega = 0.5$. The system reaches a spatially localized steady state in long time. The expectation values of the cavity particle number operators $\langle \hat{n}_j(t) \rangle$ in the course of time evolution in the first-order cumulant expansion (i.e., mean field) for (a) $j_0 = 0$ and (b) $j_0 = 5$. (c) The time evolution of the expectation value of the total photon number operator $\langle \hat{N} \rangle$ for $j_0 = 0$ in both first- and second-order cumulant expansion. (d) The distribution of $\langle \hat{n}_j(t_f) \rangle$ over lattice sites in the stationary state for $j_0 = 0$ (cf. panel a). To a very good approximation, the distribution is proportional to the probability density of a single WS state (see also Fig. 2), signalling a nonequilibrium photon Bose-condensation into a WS state. Mean field is quite accurate in this weakly interacting regime.

to disorder-free many-body localization [44, 45] (for related experiments see Ref. [46]). The second line of the Hamiltonian (1) introduces a coherent photon pumping, which along with the photon decay into the environment κ [see Eq. (3)] explicitly breaks the $U(1)$ symmetry of the system associated with the particle number conservation [43]. In the following we will show that this lack of the particle conservation and explicitly broken $U(1)$ symmetry due to the loss and gain processes has fundamental consequences in both static and dynamics of the system.

Consequences of explicit $U(1)$ symmetry breaking: State selection.—In order to gain some physical intuition, let us start with the non-interacting limit, $\chi = 0$. In the WS basis, the Heisenberg equations of motions read [43],

$$i \frac{d\hat{b}_n}{dt} = (\Delta_n - i\kappa) \hat{b}_n + \tilde{\eta}_n, \quad (4)$$

where $\hat{b}_n = \sum_j \beta_{n,j} \hat{a}_n$, $\tilde{\eta}_n = \sum_j \beta_{n,j} \eta_j$, and $\beta_{n,j} = \mathcal{J}_{j-n}(2J/\Delta\omega)$, with \mathcal{J}_k being the Bessel function of the first kind of order k . The equations of motion (4) readily yield

$$\hat{b}_n(t) = e^{-it(\Delta_n - i\kappa)} \hat{b}_n(0) + \frac{e^{-it(\Delta_n - i\kappa)} - 1}{\Delta_n - i\kappa} \tilde{\eta}_n. \quad (5)$$

If $\forall_n \tilde{\eta}_n = 0$, the solutions correspond to damped Bloch oscillations [43]. If additionally $\kappa = 0$, one then recovers the common Bloch oscillations and the choice of j_0 in Eq. (2) becomes arbitrary as it only adds an irrelevant phase factor.

In the long-time limit $t \gg \kappa^{-1} \gg J^{-1}$, regardless of the choice of initial conditions $\hat{b}_n(0)$, the Bloch oscillations are completely damped out and the system reaches a steady state with the WS mode occupations,

$$\langle \hat{n}_n \rangle = \frac{\tilde{\eta}_n^2}{(\Delta\omega)^2(n - j_0)^2 + \kappa^2}. \quad (6)$$

As can be seen from Eq. (6), now j_0 plays an essential role. In particular, by properly choosing $j_0 \in \mathbb{Z}$ one can select dynamically a single WS mode ($n = j_0$) to be microscopically occupied. However, we note this approach does not work when $\tilde{\eta}_{j_0} = 0$, which happens for some specific ratios of $J/\Delta\omega$. In these cases, one encounters a sequence of pumping anti-resonances, which lead to the occupation a few adjacent WS states instead. Furthermore, these anti-resonances are responsible for non-trivial phase boundaries between stationary and non-stationary states as shown in Fig. 3, which we will delve into it in the last section.

The above simple analysis is valid qualitatively also for sufficiently small photon-photon interactions, which we confirm numerically in the following. In numerical simulations we set $J = \hbar = 1$ (as the unit of energy), $\kappa = 10^{-2}$, $\forall_j \hat{a}_j(0) = 0$, and calculate the expectation values of the relevant operators using the cumulant expansion in both first (i.e., mean-field) and second order [43, 47]. Moreover, for the sake of simplicity and without loss of generality, we consider only a single cavity pumping $\eta_j = \eta \delta_{j,0}$, but different choices do not change our main conclusions [43]. Finally, with the exception of Fig. 1, we also fix $j_0 = 0$.

Nonequilibrium photon condensation in the weakly interacting regime.—Now, we turn our attention to the weakly interacting regime, $\chi \ll 1$. As in the non-interacting case, in the weakly interacting regime the many-photon system still occupies macroscopically a single or a few one-particle WS states with a high degree of coherence. In Fig. 1, we show the expectation value of cavity photon-number operators $\hat{n}_j = \hat{a}_j^\dagger \hat{a}_j$ as well as the total photon-number operator $\hat{N} = \sum_j \hat{n}_j$. As can be seen, in each case the system reaches a spatially-localised stationary steady state which, for the chosen parameters, is proportional to a single WS state with $n = j_0$.

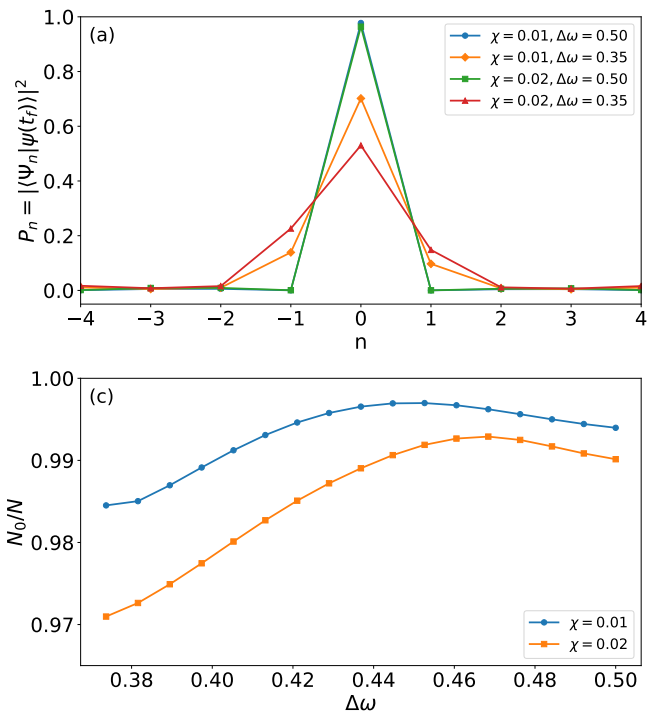


FIG. 2. (a) Steady-state fidelity $P_n(t_f)$ between the mean-field wavefunction $|\psi(t_f)\rangle$ and the WS basis states $|\Psi_n\rangle$. To a very good approximation, the condensate wavefunction is either proportional to only one WS state or is a superposition of a few WS states as in an anti-resonant case (see the discussion in the main text). (b) The dominant eigenvalue N_0 of the single-particle density matrix as a function of $\Delta\omega$ remains close to the total number of photons N , indicating a high condensate fraction.

To further quantify this observation, we calculate the fidelity $P_n(t) = |\langle \Psi_n | \psi(t) \rangle|^2$ between the mean-field wavefunction $|\psi(t)\rangle$ and the WS basis states $|\Psi_n\rangle$. The distribution of P_n is illustrated in Fig. 2(a) in steady states, showing it is centered around $n = j_0 = 0$ [cf. Eq. (6)]. In general two distinct scenarios are possible: (i) The mean-field wavefunction consists predominantly of a single WS state, or (ii) it has contributions from a few different WS states. As Fig. 2(a) shows, for $\Delta\omega = 0.5$ [as in Fig. 1(a) and (d)] the wavefunction is close to the central WS state, while for $\Delta\omega = 0.35$ two additional modes $n = \pm 1$ are also significantly occupied at the macroscopic level. This is because of the aforementioned pumping anti-resonances, where the population of $n = \pm 1$ ($n = 0$) mode is completely suppressed at $\Delta\omega \approx 0.522$ ($\Delta\omega \approx 0.362$) due to the hitting a zero of the \mathcal{J}_1 (\mathcal{J}_0) Bessel function.

In order to confirm that photons are Bose condensed, we consider the single-particle reduced density matrix $\hat{\rho}_1(x, x') = \langle \psi^\dagger(x) \psi(x') \rangle$, whose eigenvalues determine the occupation probabilities of the natural orbitals [48]. The highest occupation number quantifies the level of co-

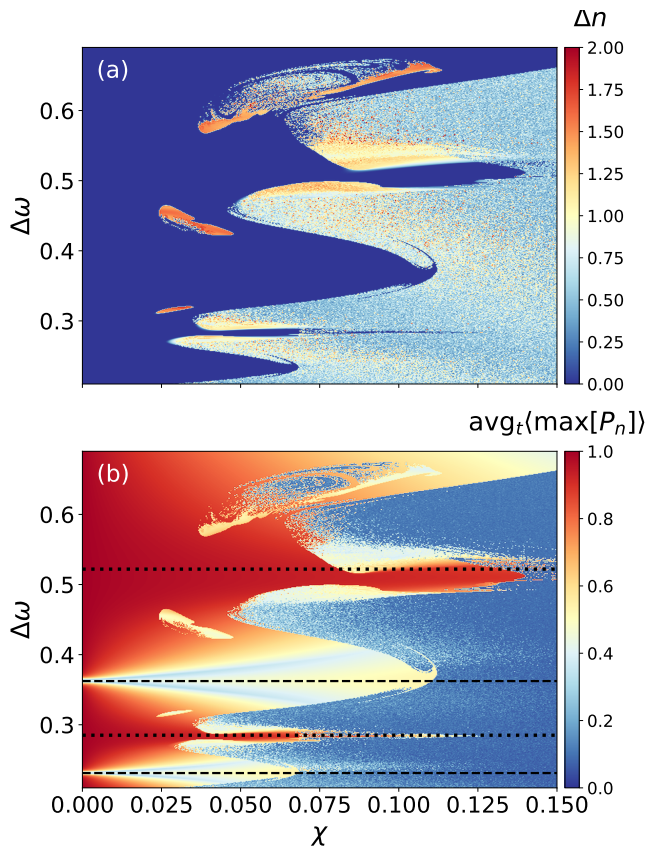


FIG. 3. Mean-field nonequilibrium many-body phase diagram of the system in the parameter plane of the force $\Delta\omega$ vs. the photon-photon interaction strength χ . (a) Relative change of the total photon number over a long-time evolution Δn [Eq. (7)] reveals three regimes: stationary steady-state phase (deep blue), dynamically unstable chaotic regime (light blue), and non-stationary regular oscillatory states (warm colors). (b) Time-averaged maximal fidelity between the mean-field wavefunction $|\psi\rangle$ and the WS basis states $|\Psi_n\rangle$ is complementary to panel (a) and reveals particularly a series of narrow bands that can be explained on a single-particle level as pumping anti-resonances; see the discussion in the main text. The dashed (dotted) lines correspond to zeros of the Bessel function \mathcal{J}_0 (\mathcal{J}_1). Note that interactions slightly shift the positions of the anti-resonances.

herence in the system. Although we can expand the field operators in any orthogonal basis, we choose the Wannier basis $\hat{\psi}(x) = \sum_j w_j(x)\hat{a}_j$ and calculate the eigenvalues of $\langle \hat{a}_j^\dagger \hat{a}_l \rangle$ in a steady state of the system in the second-order cumulant expansion [43]. Indeed, as can be seen from Fig. 2(b) the highest eigenvalue N_0 is very close to the total number of photons $N = \langle \hat{N} \rangle$, supporting the interpretation of a photon BEC. In contrast to the distribution of P_n as shown in Fig. 2(a), the highest eigenvalue of the reduced density matrix is only weakly affected by the lattice tilt $\Delta\omega$. Hence, we infer that the condensate wavefunction is either close to a single WS states or is a superposition of a few WS states.

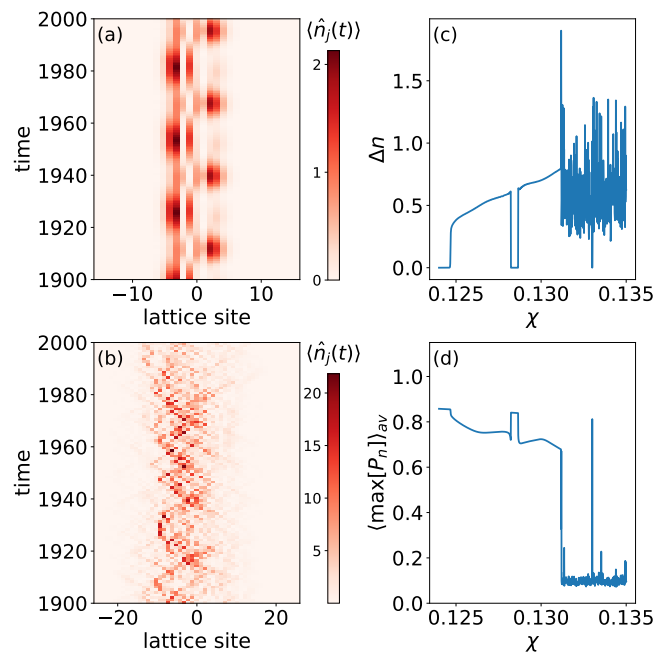


FIG. 4. Mean-field dynamics of the expectation values of the cavity photon number operators $\langle \hat{n}_j(t) \rangle$ for different interaction strengths: (a) $\chi = 0.13$ in the oscillatory regime, and (b) $\chi = 0.135$ in the chaotic regime. Stationary and different non-stationary solutions are distinguished by monitoring (c) the relative change of the total photon number over a long-time evolution and (d) the time-averaged maximal fidelity. The lattice tilt is set to $\Delta\omega = 0.5$ for all panels.

Non-stationary phases in the strongly interacting regime.—Above we showed that in the non-interacting and weakly interacting regimes photons can condensate into a one or a few selected WS states and reach a steady state. However, with increasing the interaction strength χ , the stationary states lose their stability and intriguing non-stationary solutions appear. Figure 3(a) depicts the nonequilibrium many-body phase diagram of the system in the parameter plane of $\{\chi, \Delta\omega\}$ and contains three main regimes: stationary steady states (deep blue), dynamically unstable chaotic regime (light blue), and non-stationary regular oscillatory states (warm colors). The three phases are distinguished by the relative change of the total photon number over a long-time evolution, defined as

$$\Delta n = \frac{\max_t \langle \hat{N}(t) \rangle - \min_t \langle \hat{N}(t) \rangle}{\text{avg}_t \langle \hat{N}(t) \rangle}, \quad (7)$$

with \max_t , \min_t , and avg_t denoting, respectively, the maximal, minimal, and average value of a quantum-averaged observable during a long-time evolution (where the initial transient dynamics of the system has been neglected). Although the phase diagram is dominated by the stationary and dynamically unstable chaotic regimes, regions of regular oscillatory dynamics appear mostly on

boundaries between the two regimes; see also Fig. 3(b) showing the time-averaged maximal fidelity and Supplemental Material [43].

Interestingly, photons in the regular oscillatory regime tunnel between a few neighboring cavities performing spatially-confined oscillations reminiscent of standard Bloch oscillations; see Fig. 4. Unlike standard Bloch oscillations that tend to decay in interacting systems [32–36], in our driven-dissipative model oscillatory solutions are in fact induced by the on-site photon-photon interactions and persist over long time dynamics. These solutions can be conceptualized as multimode limit cycles (as shown in Supplemental Material [43]) within driven-dissipative systems, where the steady-state solutions of equations of motion exhibit dynamic instability [49–57].

Summary, conclusions, and perspectives.—In summary, we have studied an array of coupled Kerr cavities with linearly increasing resonant cavity frequencies, which is equivalent to a $U(1)$ -symmetry broken driven-dissipative Bose-Hubbard model with a tilted potential. The model reveals a range of both stationary and non-stationary nonequilibrium phenomena. Notably, photons condense into selected, stationary WS states under sufficiently weak on-site interactions. As the strength of photon-photon interactions increases, we observe a transition to a non-stationary dynamical regime marked by periodic Bloch-like oscillations over time. Unlike the equilibrium counterpart, these regular oscillations are induced by the photon-photon interactions and do not decay over time.

Our research sheds light on the intricate behavior of driven-dissipative coupled cavity systems, emphasizing the role of explicit $U(1)$ symmetry breaking and interactions in shaping their dynamics. These findings hold promise for applications such as coherent light storage [58–60], light confinement [61–63], generation of non-classical many-photon states [64–66], and distributed quantum sensing [67–69]. While our focus in this Letter has been on weakly interacting systems, we underscore the importance of delving deeper into dynamics beyond perturbation regimes. Specifically, it is interesting to explore the non-stationary states in many-body regimes, particularly in the context of ergodicity breaking [70, 71] and Stark many-body localization [72]. Another intriguing scenario is to extend our driven-dissipative model to topological setting, where exotic nonequilibrium topological effects are expected to appear [73–76].

The data presented in this article is available from [77].

We acknowledge stimulating discussions with Darrick Chang and Thomas Pohl. This research was funded in whole or in part by the Austrian Science Fund (FWF) [grant DOIs: 10.55776/ESP171, 10.55776/M3304 and 10.55776/P35891]. For open access purposes, the authors have applied a CC BY public copyright license to any author accepted manuscript version arising from this submission. F. M. additionally acknowledges the support

of the ESQ-Discovery Grant of the Austrian Academy of Sciences (ÖAW).

-
- [1] D. Bohm, *Quantum Theory*, Dover Books on Physics (Dover Publications, Mineola, NY, 1989).
 - [2] D. F. Walls and G. F. Milburn, *Quantum Optics* (Springer Berlin Heidelberg, 2008).
 - [3] H. Deng, H. Haug, and Y. Yamamoto, Exciton-polariton Bose-Einstein condensation, *Rev. Mod. Phys.* **82**, 1489 (2010).
 - [4] J. Keeling and N. G. Berloff, Exciton-polariton condensation, *Contemp. Phys.* **52**, 131–151 (2011).
 - [5] T. Byrnes, N. Y. Kim, and Y. Yamamoto, Exciton-polariton condensates, *Nat. Phys.* **10**, 803–813 (2014).
 - [6] F. Mivehvar, F. Piazza, T. Donner, and H. Ritsch, Cavity QED with quantum gases: new paradigms in many-body physics, *Adv. Phys.* **70**, 1 (2021).
 - [7] I. Carusotto and C. Ciuti, Quantum fluids of light, *Rev. Mod. Phys.* **85**, 299 (2013).
 - [8] H. Deng, G. Weihs, C. Santori, J. Bloch, and Y. Yamamoto, Condensation of semiconductor microcavity exciton polaritons, *Science* **298**, 199–202 (2002).
 - [9] J. Kasprzak, M. Richard, S. Kundermann, A. Baas, P. Jeambrun, J. M. J. Keeling, F. M. Marchetti, M. H. Szymańska, R. André, J. L. Staehli, V. Savona, P. B. Littlewood, B. Deveaud, and L. S. Dang, Bose-Einstein condensation of exciton polaritons, *Nature* **443**, 409–414 (2006).
 - [10] R. Balili, V. Hartwell, D. Snoke, L. Pfeiffer, and K. West, Bose-Einstein Condensation of Microcavity Polaritons in a Trap, *Science* **316**, 1007–1010 (2007).
 - [11] A. Amo, J. Lefrère, S. Pigeon, C. Adrados, C. Ciuti, I. Carusotto, R. Houdré, E. Giacobino, and A. Bramati, Superfluidity of polaritons in semiconductor microcavities, *Nat. Phys.* **5**, 805–810 (2009).
 - [12] J. Klaers, J. Schmitt, F. Vewinger, and M. Weitz, Bose-Einstein condensation of photons in an optical microcavity, *Nature* **468**, 545–548 (2010).
 - [13] C. Noh and D. G. Angelakis, Quantum simulations and many-body physics with light, *Rep. Prog. Phys.* **80**, 016401 (2016).
 - [14] M. J. Hartmann, Quantum simulation with interacting photons, *J. Opt.* **18**, 104005 (2016).
 - [15] M. J. Hartmann, F. G. S. L. Brandão, and M. B. Plenio, Strongly interacting polaritons in coupled arrays of cavities, *Nat. Phys.* **2**, 849–855 (2006).
 - [16] A. D. Greentree, C. Tahan, J. H. Cole, and L. C. L. Hollenberg, Quantum phase transitions of light, *Nat. Phys.* **2**, 856–861 (2006).
 - [17] M. Hartmann, F. Brandão, and M. Plenio, Quantum many-body phenomena in coupled cavity arrays, *Laser & Photon. Rev.* **2**, 527–556 (2008).
 - [18] S. Schmidt and G. Blatter, Strong Coupling Theory for the Jaynes-Cummings-Hubbard Model, *Phys. Rev. Lett.* **103**, 086403 (2009).
 - [19] A. Tomadin, V. Giovannetti, R. Fazio, D. Gerace, I. Carusotto, H. E. Türeci, and A. Imamoglu, Signatures of the superfluid-insulator phase transition in laser-driven dissipative nonlinear cavity arrays, *Phys. Rev. A*

- 81**, 061801 (2010).
- [20] C.-W. Wu, M. Gao, Z.-J. Deng, H.-Y. Dai, P.-X. Chen, and C.-Z. Li, Quantum phase transition of light in a one-dimensional photon-hopping-controllable resonator array, *Phys. Rev. A* **84**, 043827 (2011).
- [21] Although these models share many similarities, such as bosons hopping coherently between nearest-neighbor sites with local nonlinearities, we note that quantitative differences may arise on different energy scales.
- [22] A. Le Boité, G. Orso, and C. Ciuti, Steady-State Phases and Tunneling-Induced Instabilities in the Driven Dissipative Bose-Hubbard Model, *Phys. Rev. Lett.* **110**, 233601 (2013).
- [23] A. Le Boité, G. Orso, and C. Ciuti, Bose-Hubbard model: Relation between driven-dissipative steady states and equilibrium quantum phases, *Phys. Rev. A* **90**, 063821 (2014).
- [24] T. Graß, Excitations and correlations in the driven-dissipative Bose-Hubbard model, *Phys. Rev. A* **99**, 043607 (2019).
- [25] L. Lu, J. D. Joannopoulos, and M. Soljačić, Topological photonics, *Nat. Photon* **8**, 821–829 (2014).
- [26] T. Ozawa, H. M. Price, A. Amo, N. Goldman, M. Hafezi, L. Lu, M. C. Rechtsman, D. Schuster, J. Simon, O. Zeitler, and I. Carusotto, Topological photonics, *Rev. Mod. Phys.* **91**, 015006 (2019).
- [27] G. H. Wannier, Wave Functions and Effective Hamiltonian for Bloch Electrons in an Electric Field, *Phys. Rev.* **117**, 432 (1960).
- [28] T. Hartmann, F. Keck, H. J. Korsch, and S. Mossmann, Dynamics of Bloch oscillations, *New J. Phys.* **6**, 2–2 (2004).
- [29] U. Peschel, T. Pertsch, and F. Lederer, Optical Bloch oscillations in waveguide arrays, *Opt. Lett.* **23**, 1701 (1998).
- [30] R. Sapienza, P. Costantino, D. Wiersma, M. Ghulinyan, C. J. Oton, and L. Pavesi, Optical Analogue of Electronic Bloch Oscillations, *Phys. Rev. Lett.* **91**, 263902 (2003).
- [31] L. Yuan and S. Fan, Bloch oscillation and unidirectional translation of frequency in a dynamically modulated ring resonator, *Optica* **3**, 1014 (2016).
- [32] A. Buchleitner and A. R. Kolovsky, Interaction-Induced Decoherence of Atomic Bloch Oscillations, *Phys. Rev. Lett.* **91**, 253002 (2003).
- [33] M. Gustavsson, E. Haller, M. J. Mark, J. G. Danzl, G. Rojas-Kopeinig, and H.-C. Nägerl, Control of Interaction-Induced Dephasing of Bloch Oscillations, *Phys. Rev. Lett.* **100**, 080404 (2008).
- [34] D. O. Krimer, R. Khomeriki, and S. Flach, Delocalization and spreading in a nonlinear Stark ladder, *Phys. Rev. E* **80**, 036201 (2009).
- [35] M. Eckstein and P. Werner, Damping of Bloch Oscillations in the Hubbard Model, *Phys. Rev. Lett.* **107**, 186406 (2011).
- [36] However, note that bound states of a few strongly interacting particles can experience fractional Bloch oscillations at frequencies that are multiples of single-particle Bloch oscillations [78–81] (for experiments see [82, 83]). Also, the decay of Bloch oscillations and the emergence of the directional motion in the excitation-phonon has been recently reported in [84].
- [37] A. A. Houck, H. E. Türeci, and J. Koch, On-chip quantum simulation with superconducting circuits, *Nat. Phys.* **8**, 292–299 (2012).
- [38] J. Jin, D. Rossini, R. Fazio, M. Leib, and M. J. Hartmann, Photon Solid Phases in Driven Arrays of Nonlinearly Coupled Cavities, *Phys. Rev. Lett.* **110**, 163605 (2013).
- [39] J. Jin, D. Rossini, M. Leib, M. J. Hartmann, and R. Fazio, Steady-state phase diagram of a driven QED-cavity array with cross-Kerr nonlinearities, *Phys. Rev. A* **90**, 023827 (2014).
- [40] A. Majumdar, A. Rundquist, M. Bajcsy, V. D. Dasika, S. R. Bank, and J. Vučković, Design and analysis of photonic crystal coupled cavity arrays for quantum simulation, *Phys. Rev. B* **86**, 195312 (2012).
- [41] G. Lepert, M. Trupke, M. J. Hartmann, M. B. Plenio, and E. A. Hinds, Arrays of waveguide-coupled optical cavities that interact strongly with atoms, *New J. Phys.* **13**, 113002 (2011).
- [42] A. J. Kollár, A. T. Papageorge, K. Baumann, M. A. Armen, and B. L. Lev, An adjustable-length cavity and bose–einstein condensate apparatus for multimode cavity qed, *New J. Phys.* **17**, 043012 (2015).
- [43] See Supplemental Materials for the derivation of the rotating frame Hamiltonian, discussion of Wannier-Stark states and the U(1) symmetry breaking terms, details of the cumulant expansion, and more examples of interaction-induced Bloch oscillations.
- [44] R. Yao and J. Zakrzewski, Many-body localization of bosons in an optical lattice: Dynamics in disorder-free potentials, *Phys. Rev. B* **102**, 104203 (2020).
- [45] S. R. Taylor, M. Schulz, F. Pollmann, and R. Moessner, Experimental probes of Stark many-body localization, *Phys. Rev. B* **102**, 054206 (2020).
- [46] W. Morong, F. Liu, P. Becker, K. S. Collins, L. Feng, A. Kyprianidis, G. Pagano, T. You, A. V. Gorshkov, and C. Monroe, Observation of Stark many-body localization without disorder, *Nature* **599**, 393–398 (2021).
- [47] D. Plankensteiner, C. Hotter, and H. Ritsch, Quantum-Cumulants.jl: A Julia framework for generalized mean-field equations in open quantum systems, *Quantum* **6**, 617 (2022).
- [48] C. J. Pethick and H. Smith, *Bose–Einstein Condensation in Dilute Gases* (Cambridge University Press, 2008).
- [49] F. Piazza and H. Ritsch, Self-Ordered Limit Cycles, Chaos, and Phase Slippage with a Superfluid inside an Optical Resonator, *Phys. Rev. Lett.* **115**, 163601 (2015).
- [50] C.-K. Chan, T. E. Lee, and S. Gopalakrishnan, Limit-cycle phase in driven-dissipative spin systems, *Phys. Rev. A* **91**, 051601 (2015).
- [51] E. T. Owen, J. Jin, D. Rossini, R. Fazio, and M. J. Hartmann, Quantum correlations and limit cycles in the driven-dissipative Heisenberg lattice, *New J. Phys.* **20**, 045004 (2018).
- [52] H. Keßler, J. G. Cosme, M. Hemmerling, L. Mathey, and A. Hemmerich, Emergent limit cycles and time crystal dynamics in an atom-cavity system, *Phys. Rev. A* **99**, 053605 (2019).
- [53] E. Colella, A. Kosior, F. Mivehvar, and H. Ritsch, Open Quantum System Simulation of Faraday’s Induction Law via Dynamical Instabilities, *Phys. Rev. Lett.* **128**, 070603 (2022).
- [54] P. Gao, Z.-W. Zhou, G.-C. Guo, and X.-W. Luo, Self-organized limit cycles in red-detuned atom-cavity systems, *Phys. Rev. A* **107**, 023311 (2023).
- [55] A. Kosior, H. Ritsch, and F. Mivehvar, Nonequilibrium phases of ultracold bosons with cavity-induced dynamic gauge fields, *SciPost Phys.* **15**, 046 (2023).

- [56] F. Mivehvar, Conventional and Unconventional Dicke Models: Multistabilities and Nonequilibrium Dynamics, *Phys. Rev. Lett.* **132**, 073602 (2024).
- [57] J. Skulte, P. Kongkhambut, H. Keßler, A. Hemmerich, L. Mathey, and J. G. Cosme, Realizing limit cycles in dissipative bosonic systems (2024), [arXiv:2401.05332 \[cond-mat.quant-gas\]](https://arxiv.org/abs/2401.05332).
- [58] D. F. Phillips, A. Fleischhauer, A. Mair, R. L. Walsworth, and M. D. Lukin, Storage of Light in Atomic Vapor, *Phys. Rev. Lett.* **86**, 783 (2001).
- [59] Y. O. Dudin, L. Li, and A. Kuzmich, Light storage on the time scale of a minute, *Phys. Rev. A* **87**, 031801 (2013).
- [60] O. Katz and O. Firstenberg, Light storage for one second in room-temperature alkali vapor, *Nat. Commun* **9**, 2074 (2018).
- [61] H. Cao, J. Y. Xu, D. Z. Zhang, S.-H. Chang, S. T. Ho, E. W. Seelig, X. Liu, and R. P. H. Chang, Spatial confinement of laser light in active random media, *Phys. Rev. Lett.* **84**, 5584 (2000).
- [62] M. Notomi, Strong light confinement with periodicity, *Proc. IEEE* **99**, 1768 (2011).
- [63] F. Riboli, N. Caselli, S. Vignolini, F. Intonti, K. Vynck, P. Barthelémy, A. Gerardino, L. Balet, L. H. Li, A. Fiore, M. Gurioli, and D. S. Wiersma, Engineering of light confinement in strongly scattering disordered media, *Nat. Mater* **13**, 720 (2014).
- [64] M. Cooper, L. J. Wright, C. Söller, and B. J. Smith, Experimental generation of multi-photon Fock states, *Opt. Express* **21**, 5309 (2013).
- [65] D. E. Chang, V. Vuletić, and M. D. Lukin, Quantum nonlinear optics—photon by photon, *Nat. Photon* **8**, 685 (2014).
- [66] A. Pizzi, A. Gorlach, N. Rivera, A. Nunnenkamp, and I. Kaminer, Light emission from strongly driven many-body systems, *Nat. Phys* **19**, 551 (2023).
- [67] X. Guo, C. R. Breum, J. Borregaard, S. Izumi, M. V. Larsen, T. Gehring, M. Christandl, J. S. Neergaard-Nielsen, and U. L. Andersen, Distributed quantum sensing in a continuous-variable entangled network, *Nature Physics* **16**, 281 (2020).
- [68] Z. Zhang and Q. Zhuang, Distributed quantum sensing, *Quantum Sci. Technol.* **6**, 043001 (2021).
- [69] J. C. Pelayo, K. Gietka, and T. Busch, Distributed quantum sensing with optical lattices, *Phys. Rev. A* **107**, 033318 (2023).
- [70] A. D. Luca and A. Scardicchio, Ergodicity breaking in a model showing many-body localization, *Europhys Lett.* **101**, 37003 (2013).
- [71] K. Gietka, J. Chwedeńczuk, T. Wasak, and F. Piazza, Multipartite entanglement dynamics in a regular-to-ergodic transition: Quantum fisher information approach, *Phys. Rev. B* **99**, 064303 (2019).
- [72] M. Schulz, C. A. Hooley, R. Moessner, and F. Pollmann, Stark many-body localization, *Phys. Rev. Lett.* **122**, 040606 (2019).
- [73] M. Hafezi, S. Mittal, J. Fan, A. Migdall, and J. M. Taylor, Imaging topological edge states in silicon photonics, *Nat. Photon* **7**, 1001–1005 (2013).
- [74] S. Mittal, J. Fan, S. Faez, A. Migdall, J. M. Taylor, and M. Hafezi, Topologically robust transport of photons in a synthetic gauge field, *Phys. Rev. Lett.* **113**, 087403 (2014).
- [75] Z. Gong, Y. Ashida, K. Kawabata, K. Takasan, S. Higashikawa, and M. Ueda, Topological phases of non-hermitian systems, *Phys. Rev. X* **8**, 031079 (2018).
- [76] E. Colella, F. Mivehvar, F. Piazza, and H. Ritsch, Hofstadter butterfly in a cavity-induced dynamic synthetic magnetic field, *Phys. Rev. B* **100**, 224306 (2019).
- [77] A. Kosior, K. Gietka, F. Mivehvar, and H. Ritsch, *Dynamical photon condensation into wannier-stark states*.
- [78] F. Claro, J. F. Weisz, and S. Curilef, Interaction-induced oscillations in correlated electron transport, *Phys. Rev. B* **67**, 193101 (2003).
- [79] W. S. Dias, E. M. Nascimento, M. L. Lyra, and F. A. B. F. de Moura, Frequency doubling of Bloch oscillations for interacting electrons in a static electric field, *Phys. Rev. B* **76**, 155124 (2007).
- [80] R. Khomeriki, D. O. Krimer, M. Haque, and S. Flach, Interaction-induced fractional Bloch and tunneling oscillations, *Phys. Rev. A* **81**, 065601 (2010).
- [81] D. Wiater, T. Sowiński, and J. Zakrzewski, Two bosonic quantum walkers in one-dimensional optical lattices, *Phys. Rev. A* **96**, 043629 (2017).
- [82] G. Corrielli, A. Crespi, G. Della Valle, S. Longhi, and R. Osellame, Fractional Bloch oscillations in photonic lattices, *Nat. Commun* **4**, 1555 (2013).
- [83] P. M. Preiss, R. Ma, M. E. Tai, A. Lukin, M. Rispoli, P. Zupancic, Y. Lahini, R. Islam, and M. Greiner, Strongly correlated quantum walks in optical lattices, *Science* **347**, 1229–1233 (2015).
- [84] A. Kosior, S. Kokkelmans, M. Lewenstein, J. Zakrzewski, and M. Płodzień, Phonon-assisted coherent transport of excitations in Rydberg-dressed atom arrays, *Phys. Rev. A* **108**, 043308 (2023).

SUPPLEMENTAL MATERIAL

Derivation of the rotation frame Hamiltonian

Consider an array of optical Kerr cavities labeled by $j = -L/2, \dots, L/2$. Each cavity in the array is assumed to have a distinct primary mode with a unique frequency denoted as ω_j . The neighboring cavities are coupled through photon exchange, described as a nearest-neighbor tunneling process, where a photon leaks out of one cavity and enters the adjacent one. The full Hamiltonian in the lab frame is given by

$$\hat{H}_{\text{Lab}} = -J \sum_j \left(\hat{a}_j^\dagger \hat{a}_{j+1} + \text{H.c.} \right) + \sum_j \omega_j \hat{a}_j^\dagger \hat{a}_j + \chi \sum_j \hat{a}_j^{\dagger 2} \hat{a}_j^2 + \sum_j \eta_j \left(\hat{a}_j e^{i\omega_p t} + \hat{a}_j^\dagger e^{-i\omega_p t} \right), \quad (\text{S1})$$

where $\hat{a}_j, \hat{a}_j^\dagger$ are bosonic operators for annihilating and creating photons in the j -th cavity with frequency $\omega_j = \omega_0 + j\Delta\omega$. Here, J is the tunneling amplitude, χ is the Kerr non-linearity leading to on-site photon-photon interaction, and η_j is the pumping rate of the j th cavity with a pumping laser of frequency ω_p .

To switch to a rotating frame with slowly varying variables, a unitary transformation with a time-dependent operator is applied

$$U(t) = \prod_j \exp \left(i\omega_p t \hat{a}_j^\dagger \hat{a}_j \right), \quad (\text{S2})$$

transforming the bosonic operators to $\hat{a}'_j = U \hat{a}_j U^\dagger = \exp(-i\omega_p t) \hat{a}_j$ and the Hamiltonian to $\hat{H} = U \hat{H}_{\text{Lab}} U^\dagger + i(\partial_t U) U^\dagger$, i.e.,

$$\hat{H} = -J \sum_j \left(\hat{a}'_j \hat{a}'_{j+1} + \text{H.c.} \right) + \sum_j \Delta_j \hat{a}'_j \hat{a}'_j + \chi \sum_j \hat{a}'_j^{\dagger 2} \hat{a}'_j{}^2 + \sum_j \eta_j \left(\hat{a}_j + \hat{a}'_j \right), \quad (\text{S3})$$

where $\Delta_j = \Delta\omega (j - j_0)$ with $j_0 = (\omega_p - \omega_0)/\Delta\omega$.

Bloch oscillations and consequences of U(1) symmetry

Here, for pedagogical reasons, we first consider a non-interacting bosonic Hamiltonian in a tilted potential and show the system exhibits Bloch oscillations. Then, we introduce a pumping term $\sum_j \eta_j \left(\hat{a}_j + \hat{a}'_j \right)$ and discuss the consequences of U(1) symmetry breaking in weakly interacting systems.

Bloch oscillations

The non-interacting Hamiltonian of our interest reads

$$\hat{H}_0 = -J \sum_j \left(\hat{a}'_j \hat{a}'_{j+1} + \text{H.c.} \right) + \sum_j \Delta_j \hat{a}'_j \hat{a}'_j \quad (\text{S4})$$

with $\Delta_j = \Delta\omega (j - j_0)$, where the choice of j_0 is irrelevant due to the conservation of the particle number. The Hamiltonian is quadratic in \hat{a}'_j, \hat{a}_j and can be readily diagonalised by a unitary transformation

$$\hat{b}_n = \sum_{j=-\infty}^{\infty} \beta_{n,j} \hat{a}_j, \quad \beta_{n,j} = \mathcal{J}_{j-n} \left(\gamma = \frac{2J}{\Delta\omega} \right) \quad (\text{S5})$$

with \mathcal{J}_m being the Bessel function of the first kind of order m . Since the transformation is unitary, then $\beta_{n,j}$ must fulfill

$$\sum_j \beta_{n,j} \beta_{m,j} = \delta_{n,m}. \quad (\text{S6})$$

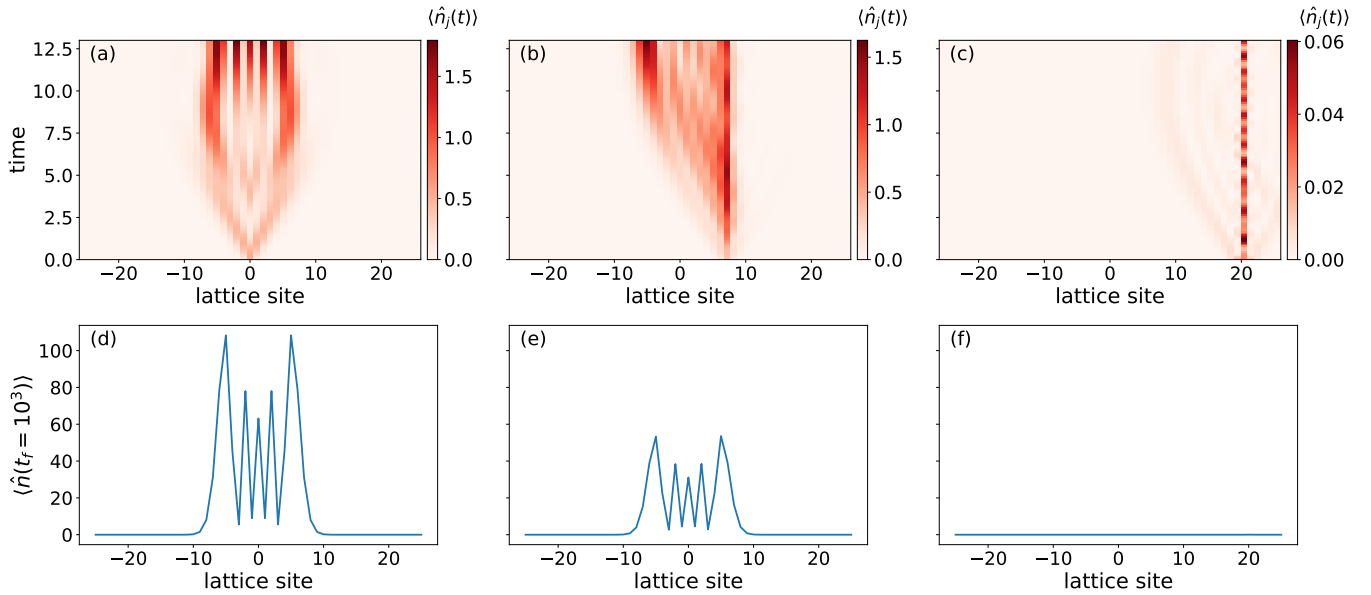


FIG. S1. (a)-(c) The expectation values of particle number operators $\langle \hat{n}_j(t) \rangle$ in early times of evolution in a very weakly interacting case with a different pumping $\eta_j = \delta_{j,j'}$: (a) $j' = 0$, (b) $j' = 7$, (c) $j' = 20$. (d)-(e) The respective site occupation distributions after long time evolution in stationary states. In all panels $j_0 = 0$, $\Delta\omega = 0.3$ and $\chi = 10^{-2}$.

Indeed, using the Bessel function addition theorem

$$\sum_m \mathcal{J}_m(x) \mathcal{J}_{n-m}(y) = \mathcal{J}_n(x+y) \quad (\text{S7})$$

as well as the property $\mathcal{J}_n(x) = \mathcal{J}_{-n}(-x)$, we obtain

$$\sum_j \mathcal{J}_{j-n}(\gamma) \mathcal{J}_{j-m}(\gamma) = \mathcal{J}_{m-n}(0) = \delta_{n,m}. \quad (\text{S8})$$

The inverse transformation then reads

$$\hat{a}_j = \sum_n \beta_{n,j} \hat{b}_n. \quad (\text{S9})$$

The eigenstates $|\Psi_n\rangle = \hat{b}_n^\dagger|0\rangle$ are called the Wannier-Stark (WS) states. In practise, the infinite summation can be truncated, as the Bessel function $\mathcal{J}_{j-n}(\gamma)$ is mainly localised in the interval $|j-n| < |\gamma|$. Although the formula holds for an infinite lattice, the WS states have finite spatial size, and therefore it can be used with a very good accuracy to describe bulk states of a finite-size lattice. Using the WS basis, the Hamiltonian (S4) can be recast into a diagonal form,

$$\hat{H}_0 = \Delta\omega \sum_n n \hat{b}_n^\dagger \hat{b}_n. \quad (\text{S10})$$

The time evolution of the Wannier state, $|j\rangle = \hat{a}_j^\dagger|0\rangle$, reads

$$|j(t)\rangle = \exp(i\hat{H}_0 t)|j\rangle = \sum_n \beta_{n,j} e^{in\Delta\omega t} |\Psi_n\rangle = \sum_{n,k} \beta_{n,j} \beta_{n,k} e^{in\Delta\omega t} |k\rangle, \quad (\text{S11})$$

which is a T -periodic function with period $T = 2\pi/\Delta\omega$. Consequently, a state which is initially maximally localised on a tilted lattice performs Bloch oscillations around the initial position.

U(1) symmetry

Because the total number of particles in the Hamiltonian \hat{H}_0 of Eq. (S4) is conserved, we were able to neglect the term $\hat{K} = -j_0 \sum_j \hat{a}_j^\dagger \hat{a}_j$, that commutes with the Hamiltonian. Equivalently, \hat{K} can be gauged out by applying the time-dependent transformation

$$V(t) = \Pi_j \exp\left(i\chi(t)\hat{a}_j^\dagger \hat{a}_j\right), \quad \chi(t) = \int^t j_0(\tau) d\tau, \quad (\text{S12})$$

where we assumed that j_0 can be explicitly time dependent. The transformation only modifies the global phase of the bosonic operators $\hat{a}'_j = V\hat{a}_j\tilde{V}^\dagger = \exp[-i\chi(t)]\hat{a}_j$ and does not contribute to the dynamics. It is a mere manifestation of the $U(1)$ symmetry of the model.

The full Hamiltonian of our system (S3), which we study in the main text, consist of two additional terms,

$$\hat{H} = \hat{H}_0 + \chi \sum_j \hat{a}_j^{\dagger 2} \hat{a}_j^2 + \sum_j \eta_j \left(\hat{a}_j + \hat{a}_j^\dagger\right), \quad (\text{S13})$$

where the first term describes contact boson-boson interactions, and the second accounts for coherent injection of bosons into the lattice. Although the interacting term is invariant under the $U(1)$ symmetry of Eq. (S12), in general it is responsible for the decay of Bloch oscillations [32–35]. The second term explicitly breaks the $U(1)$ symmetry of the model, and therefore $\hat{K} = -j_0 \sum_j \hat{a}_j^\dagger \hat{a}_j$ does not commute with \hat{H} and cannot be neglected anymore. As described in the main text, the presence of $U(1)$ symmetry breaking terms in the Hamiltonian has enormous consequences to the system's dynamics and is responsible for the dynamical photon condensation.

Additionally, in Fig. S1(a)-(c) we show the early-time evolution of expectation values of particle number operators $\langle \hat{n}_j \rangle = \langle \hat{a}_j^\dagger \hat{a}_j \rangle$ in each lattice site with different pumping schemes in the non-interacting case, while in Fig. S1(d)-(e) we show the corresponding long-time occupation numbers of photons over lattice sites. The final state is proportional to a central WS state irrespective of j' , as long as j' lies within the WS localization range, i.e., approximately, $|j'| < |\gamma|$.

Cumulant expansion

In this section, we briefly introduce the cumulant expansion method. For an open system, the time evolution of an average of an observable \hat{O} can be calculated according to

$$\frac{d\langle \hat{O} \rangle}{dt} = \frac{i}{\hbar} \langle [\hat{H}, \hat{O}] \rangle + \sum_j \kappa_j \langle 2\hat{c}_j \hat{O} \hat{c}_j^\dagger - \hat{c}_j^\dagger \hat{c}_j \hat{O} - \hat{O} \hat{c}_j^\dagger \hat{c}_j \rangle, \quad (\text{S14})$$

where κ_j characterizes the j th decay channel and c_j the corresponding jump operator. Writing down the equations explicitly, we typically find out an infinite hierarchy of equations for products of operators, which can be attributed to the non-commutativity of various operators. A well-established approach to deal with the infinite set of equations is to neglect quantum correlations. In such a case, an average value of operator product can be rewritten as product of average values of operators, $\langle \hat{O}_1 \hat{O}_2 \rangle = \langle \hat{O}_1 \rangle \langle \hat{O}_2 \rangle$, which is typically referred to as the mean field approach. More generally, it is possible to neglect quantum correlations of an arbitrary order. A systematic approach to such a truncation is realized by a so-called cumulant expansion, which relies on decomposing average values of arbitrary operator products into products of average values of operators of a given lower order, leading to a closed set of equations.

Interaction-induced Bloch oscillations

In this section we focus on interaction-induced Bloch-like oscillations, which arise in our system whenever stationary solutions are not dynamically stable, in a similarity to the limit cycle solutions in driven dissipative systems [add citations]. Indeed, these oscillations can be interpreted as multi-mode limit cycles as shown in Fig. S2(a). [On the other hand, stronger on-site interactions result in chaotic behavior, see Fig. S2(b).]

In the main text of this manuscript, we argue that the nonequilibrium phases of the system can be identified by two observables:

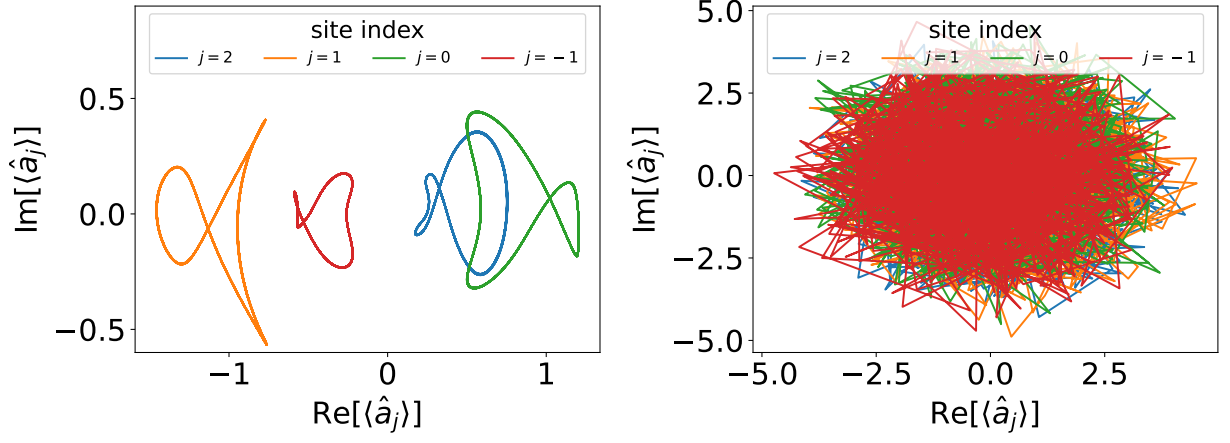


FIG. S2. Evolution of the photonic field amplitudes $\langle \hat{a}_j \rangle$ on the complex plane for $\Delta\omega = 0.5$ and (a) $\chi = 0.13$, (b) $\chi = 0.135$ [as in Fig. 4 in the main text]. (a) In the regime corresponding to the regular oscillatory behavior, the photonic fields evolve along closed trajectories. (b) In the unstable regime, photonic fields evolve chaotically. For the clarity of the presentation only selected modes are shown.

- Δn —relative change of the total photon number over a long-time evolution, defined as

$$\Delta n = \frac{\max_t \langle \hat{N}(t) \rangle - \min_t \langle \hat{N}(t) \rangle}{\text{avg}_t \langle \hat{N}(t) \rangle}, \quad (\text{S15})$$

with \max_t , \min_t and avg_t denoting maximal, minimal and the average value of an observable during a long-time evolution (where the initial transient dynamics of the system has been neglected), and

- $\langle \max[P_n(t)] \rangle_{av}$ —time-averaged maximal fidelity (i.e. square modulus of the overlap) between the mean-field wavefunction $|\psi\rangle$ and the WS basis $|\Psi_n\rangle = \hat{b}_n^\dagger |0\rangle = \sum_j \beta_{n,j} \hat{a}_j^\dagger |0\rangle$.

In order to find the stable islands of interaction-induced Bloch oscillation it is convenient to define a third observable, as a simple product of the previous two observables,

$$\Theta = \Delta n \cdot \text{avg}_t \langle \max[P_n(t)] \rangle \quad (\text{S16})$$

see Fig. S3, where we show that Θ is close to zero both in the stationary and chaotic phases, and therefore it is a good observable to identify non-stationary regular dynamics in the system.

Finally, in Fig. S4 we illustrate the expectation values of particle number operators $\langle \hat{n}_j(t) \rangle$ in the course of time evolution for different parameters of the system, showing more examples of interaction-induced oscillations.

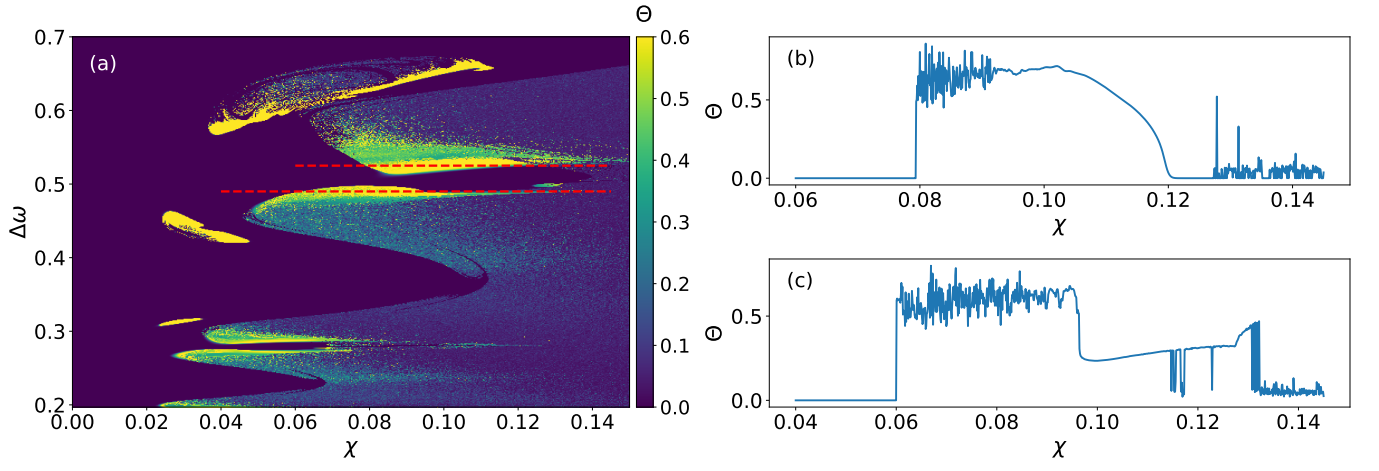


FIG. S3. The density plot of Θ which identifies stability islands of interaction-induced regular oscillations (bright colors). Panels (b) and (c) depict cuts through the density plot at the positions of red dashed lines. (b) $\Delta\omega = 0.525$, (c) $\Delta\omega = 0.49$.

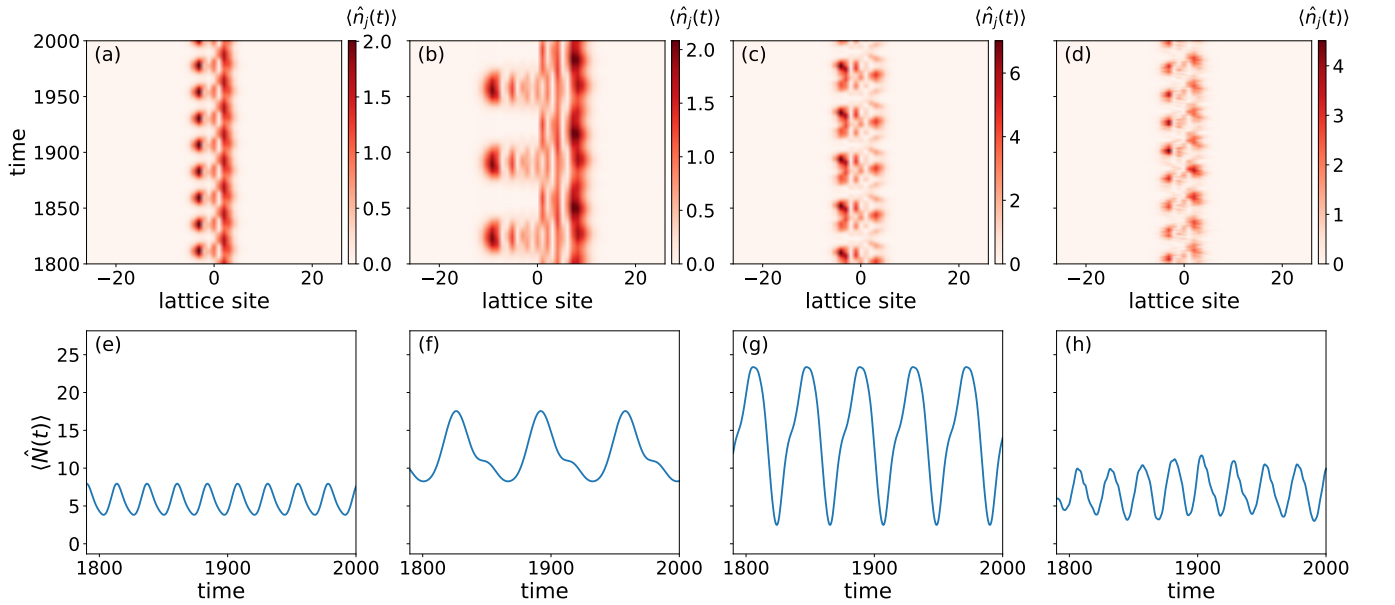


FIG. S4. Panels present the expectation values of particle number operators $\langle \hat{n}_j(t) \rangle$ in the course of time evolution showing more examples of interaction-induced oscillations for different parameters of the system. (a) $\chi = 0.11$, $\Delta\omega = 0.525$ (b) $\chi = 0.05$, $\Delta\omega = 0.2$, (c) $\chi = 0.03$, $\Delta\omega = 0.45$, (d) $\chi = 0.09$, $\Delta\omega = 0.525$. Other parameters as in the main text of this Letter.